

Prediction and Detection of Glaucomatous Visual Field Progression Using Deep Learning on Macular Optical Coherence Tomography

Jonathan Huang, BS,* Galal Galal, MD, MPH,† Vladislav Mukhin, MS,†
Mozziyar Etemadi, MD, PhD,‡‡§ and Angelo P. Tanna, MD*

Précis: A deep learning model trained on macular OCT imaging studies detected clinically significant functional glaucoma progression and was also able to predict future progression.

Objective: To use macular optical coherence tomography (OCT) imaging to predict the future and detect concurrent visual field progression, respectively, using deep learning.

Design: A retrospective cohort study.

Subjects: A pretraining data set was comprised of 7,702,201 B-scan images from 151,389 macular OCT studies. The progression detection task included 3902 macular OCT imaging studies from 1534 eyes of 828 patients with glaucoma, and the progression prediction task included 1346 macular OCT studies from 1205 eyes of 784.

Methods: A novel deep learning method was developed to detect glaucoma progression and predict future progression using macular OCT, based on self-supervised pretraining of a vision transformer (ViT) model on a large, unlabeled data set of OCT images. Glaucoma progression was defined as a mean deviation (MD) rate of change of ≤ -0.5 dB/year over 5 consecutive Humphrey visual field tests, and rapid progression was defined as MD change ≤ -1 dB/year.

Main Outcome Measures: Diagnostic performance of the ViT model for prediction of future visual field progression and detection of concurrent visual field progression using area under the receiver operating characteristic curve (AUC), sensitivity, and specificity.

Results: The model distinguished stable eyes from progressing eyes, achieving an AUC of 0.90 (95% CI, 0.88–0.91). Rapid progression was detected with an AUC of 0.92 (95% CI, 0.91–0.93). The model also demonstrated high predictive ability for forecasting future glaucoma progression, with an AUC of 0.85 (95% CI 0.83–0.87). Rapid progression was predicted with an AUC of 0.84 (95% CI 0.81–0.86).

Conclusions: A deep learning model detected clinically significant functional glaucoma progression using macular OCT imaging

studies and was also able to predict future progression. Early identification of patients undergoing glaucoma progression or at high risk for future progression may aid in clinical decision-making.

Key Words: deep learning, glaucoma, macular OCT, visual field progression

(*J Glaucoma* 2024;33:246–253)

Visions loss due to primary open angle glaucoma (POAG) is a common cause of preventable, irreversible blindness globally.¹ However, the insidious disease course and the resulting difficulty in ascertaining progression pose significant challenges to glaucoma management.² Close consideration of the individual patient's disease trajectory is needed to differentiate between stable and worsening disease. Clinical decision-making in glaucoma draws, in part, upon both structural and functional assessments through optical coherence tomography (OCT) imaging and standard automated perimetry (SAP), respectively.^{3,4} Integration of structural and functional changes across the disease course is needed to inform decisions regarding the optimal medical or surgical interventions required to maximize the likelihood of the preservation of vision.

Structural and functional measures of disease progression may not align. This is particularly important in early glaucoma before significant retinal ganglion cell (RGC) loss has occurred, as well as later in the disease process when extensive RGC loss renders evaluations of retinal nerve fiber layer (RNFL) thickness less informative.^{5–7} Moreover, measurement of functional decline with SAP is limited by inter-test variability.⁸ As a result, multiple tests are often necessary to reliably detect progression, which may contribute to delayed initiation of more intensive treatment.^{9,10} Thus, early identification of structural changes that reliably indicate ongoing functional progression is desirable to enable a more objective and reliable determination of clinically significant progression.

Macular OCT has been established as an important adjunctive imaging modality in glaucoma management.^{11,12} Due to the high density of RGCs within the macula, OCT imaging of this region has the potential to reveal early glaucomatous changes in conjunction with optic nerve head and peripapillary imaging.^{13,14} While previous studies have developed and validated deep learning methodologies analyzing fundus photography for this task,¹⁵ the use of deep learning to analyze OCT images may provide new insights linking structural and functional changes in the disease process. However, the ability of deep learning to detect and predict structural changes in macular OCT corresponding to functional progression remains to be established.

Received for publication September 23, 2023; accepted November 26, 2023.

From the *Department of Ophthalmology; †Department of Anesthesiology, Northwestern University Feinberg School of Medicine;

‡Research and Development, Northwestern Medicine Information Services, Chicago; and §Department of Biomedical Engineering, Northwestern University, Evanston, IL.

This study was supported by an unrestricted departmental grant from Research to Prevent Blindness.

Disclosure: M.E.: Cardiosense (Board member). A.P.T.: Alcon (Consultant), Apotex (Consultant), Ivantis (Consultant), and Zeiss (Consultant). The remaining authors have no conflicts to report.

Reprints: Angelo P. Tanna, MD, Department of Ophthalmology, Northwestern University Feinberg School of Medicine, 645 N. Michigan Avenue, Suite 440, Chicago, IL 60611 (e-mail: atanna@northwestern.edu).

Supplemental Digital Content is available for this article. Direct URL citations are provided in the HTML and PDF versions of this article on the journal's website, www.glaucomajournal.com.

Copyright © 2024 Wolters Kluwer Health, Inc. All rights reserved.

DOI: 10.1097/IJG.0000000000002359

One promising approach for the analysis of macular OCT images is self-supervised learning, which is similar to unsupervised learning in that it allows for model pretraining using large amounts of unlabeled data. However, in contrast to unsupervised methods, self-supervised methods independently extract information from training data. This enables the development of generalizable, task-agnostic models, which can then be adopted to different downstream prediction tasks. Vision transformer models trained using self-supervised learning have attained state-of-the-art results on image classification benchmarks,¹⁶ and there is great potential for an ophthalmology-specific pretrained model to generalize to downstream tasks such as glaucoma prediction. The aim of the present study was to examine the feasibility of using a vision transformer (ViT)-based model pretrained using a self-supervised learning method called self-distillation with no labels (DINO),¹⁶ to both predict glaucomatous visual field progression and detect concurrent visual field progression using only macular OCT images.

METHODS

Longitudinal Data Set

All data were abstracted from a deidentified, longitudinal, institutional database containing macular spectral domain OCT, Humphrey visual field (HVF), and clinical data for over 35,000 patients from 2010 to 2018. All macular OCT scans, regardless of scan range, were used for model pre-training, as detailed below. Macular OCT scans were obtained using the Spectralis platform (Heidelberg Engineering, Heidelberg, Germany). Given the scale of the data set and the demonstrated ability of self-supervised learning algorithms to learn robust image features from noisy data,¹⁷ image quality control was not performed beyond that done for initial entry into the database. HVF tests were performed using the Humphrey Field Analyzer 3 perimeter (Carl Zeiss Meditec, Dublin, CA), with the standard Swedish interactive thresholding algorithm (SITA Standard) method.

Model Pretraining Process

All available macular OCT images, with the exception of a held-out test set described below, were used to pretrain a ViT model using DINO, a method for self-supervised learning through knowledge distillation introduced by Caron et al.¹⁶ Figure 1 summarizes the DINO pretraining method. In brief, a student and a teacher ViT network are trained in parallel to unify their outputs over local and global image crops, respectively. This training process guides the models towards learning correspondences between local and global features in a self-supervised fashion. A ViT model trained in this way encodes OCT image data into a numeric form, also known as an embedding, which can then be used to perform downstream classification and prediction tasks.

Individual B-scans were resized to 384×496 using bicubic interpolation and were normalized to mean 0.5 and SD 0.5. Random contrast, brightness, and horizontal flip transformations were applied as part of the DINO image augmentation pipeline. ViT models with a hidden size of 768, 12 attention heads, 24 hidden layers, and a patch size of 8 were used for both student and teacher models. The learning rate was set to 0.0001 with a 10-epoch linear warmup. Otherwise, the default DINO hyperparameters were maintained.¹⁶ The training was performed for 20 epochs, after which the training loss reached 0.683.

All model development was performed using PyTorch version 1.13.0 and Python version 3.10.6. The training was performed on a machine with 8 80GB NVIDIA A100 graphics processing units (Nvidia Corporation, Santa Clara, California), with a training time per epoch of ~20 hours. The DINO training code is available online at <https://github.com/facebookresearch/dino>.¹⁶

To visualize the clustering capability of the pretrained ViT model, 5000 macular B-scans from patients with POAG and 5000 from patients without POAG, as defined in the “Glaucoma progression data set” section, were randomly selected and embedded using the pretrained ViT. The embeddings were reduced first to 30 dimensions using principal component analysis, then to 2 dimensions using *t*-distributed stochastic neighbor embedding (t-SNE).

Glaucoma Progression Data set

Patients with a clinical diagnosis of POAG who underwent at least 5 HVF tests were identified from the database. POAG was defined based on International Classification of Diseases codes captured in the electronic medical record and excluded glaucoma attributable to secondary causes. Clinically significant glaucoma progression was defined as a mean deviation (MD) decrease of ≤ -0.5 decibels (dB)/year over at least 5 consecutive, reliable 24-2 SITA Standard HVF tests at ≥ 6 -month intervals. Progression was further categorized as rapid (MD decrease ≤ -1.0 dB/year) or moderate (rate of MD decrease between -0.5 and -1.0 dB/year).¹⁸ HVF reliability was defined by false-positive rate $< 15\%$, false-negative rate $< 33\%$, and fixation losses $< 33\%$. Exclusion criteria were the presence of cataract with visual acuity 20/40 or worse, treatment with anti-VEGF agent, or incisional glaucoma surgery during the HVF observation period. Summary statistics were generated to describe patient demographics and disease characteristics using the mean and SD for normally distributed data and median and interquartile range for non-normally distributed data.

For each prediction task, a hold-out validation set was identified by sorting the list of unique included patients by first date of entry in the database and selecting the macular OCT studies corresponding to one-fifth of patients most recently added to the database. As classification using a model trained on retrospectively collected data is fundamentally a task of predicting the future, the date of entry to the database was used to select the hold-out validation set to mimic the temporal difference in the patient population inherent in a potential clinical evaluation.¹⁹ Model development was performed using 80/20 train/test splits on macular OCT studies from the remaining training set of patients. The DINO pretraining process was performed with OCT imaging data from these patients completely excluded.

First, the model was evaluated on the ability to classify the progression status of macular OCT imaging studies. Macular OCT studies were considered if they were obtained within 6 months of an HVF test with an additional 2 HVF tests performed before and 2 performed afterward, at intervals of ≥ 6 months (Fig. 2A). Progression status for each macular OCT study thus identified was determined using these 5 consecutive HVF tests, and a classifier was trained to output the progression status given the macular OCT study as input (see below).

The predictive value of this method for detecting new onset of visual field progression was evaluated. Patients were included if they experienced a period of no progression

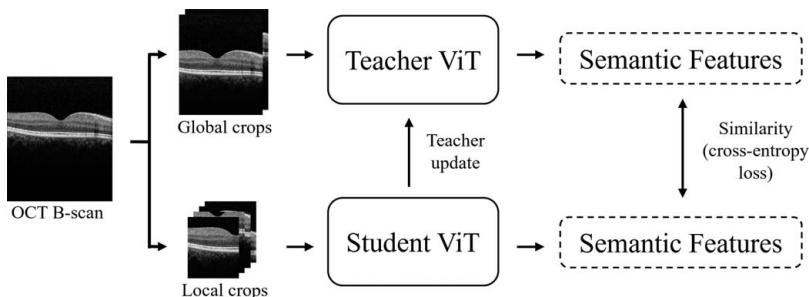


FIGURE 1. Overview of the self-supervised DINO pretraining process. Local and global crops of individual B-scans are taken and passed to a student and teacher ViT model, respectively. Both students and teachers share the same architecture. During training, cross-entropy loss is applied to the features outputted by the ViT models. The weights of the student ViT are updated by stochastic gradient descent, while the weights of the teacher ViT are updated with an exponential moving average of the student weights. Following the pretraining process, the teacher ViT is used for downstream prediction tasks. ViT indicates vision transformer.

followed by either moderate or rapid progression and if there was a macular OCT study available before the first HVF test indicating progression onset (Fig. 2B). This macular OCT was used as the classifier input. In addition, patients who experienced no progression over the entire HVF observation period were included, with each macular OCT directly preceding a period of no progression used as classifier inputs. A classifier was then trained to predict the future progression status given the input baseline macular OCT study.

Progression Classification

The macular OCT classification pipeline is described in Figure 3. To classify the progression status of macular OCT as well as to predict future glaucoma progression from a baseline macular OCT, supervised linear classifiers (comprising a single feedforward layer) were trained on the frozen ViT embeddings, in line with typical evaluations of self-supervised learning methods.¹⁶ For each B-scan, weights from the teacher ViT network pretrained using DINO were used to generate 1536-dimensional embeddings comprising the class

(CLS) token concatenated to the global average pooled patch tokens over the last ViT layer. Three output labels corresponding to no progression, moderate progression, and rapid progression were used in training the linear classifier. The fully connected linear layer was initialized with weights randomly initialized with a mean of 0 and SD of 0.01, and the bias was initialized to 0. The linear classifier was trained for 100 epochs, with a learning rate of 0.00005 selected by sweeping.

To combine predictions for an entire OCT study, the ability of models pretrained using DINO to perform unsupervised clustering¹⁶ was used to differentially weight the linear classifier outputs for individual B-scans based on their glaucoma relevance. Using K-nearest neighbors (k-NN) on the entire pretraining data set, the 20 nearest neighbors of each B-scan were used to determine the prediction probability for POAG diagnosis. For example, the prediction probability for a B-scan with 12 of the 20 nearest neighbors from patients with POAG would be 0.6. This prediction probability was used to weight the outputs of the linear classifier (after converting to probability scores using

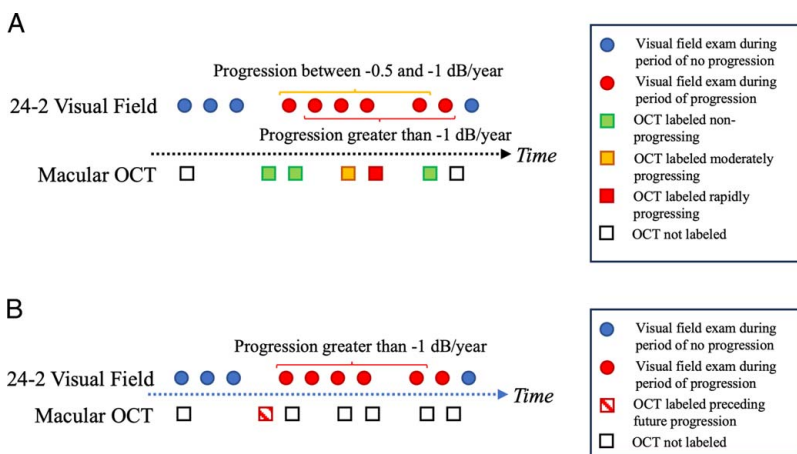


FIGURE 2. A, Progression status is determined in windows of 5 consecutive HVF tests at 6 month or greater intervals. A decrease in mean deviation (MD) of ≤ -0.5 dB/year is considered progression, and a decrease in MD of ≤ -1 dB/year is considered rapid progression; otherwise, the eye is deemed non-progressing. To assign progression status to a macular OCT, the temporally closest HVF test and its 2 preceding and 2 subsequent tests are taken as the HVF window. B, For the progression prediction task, future progression status is determined for macular OCT imaging studies obtained during a period of non-progression. The progression status of the subsequent 5 HVF tests after the macular OCT study is used as the prediction label. HVF indicates Humphrey visual field; MD, mean deviation; OCT, optical coherence tomography.

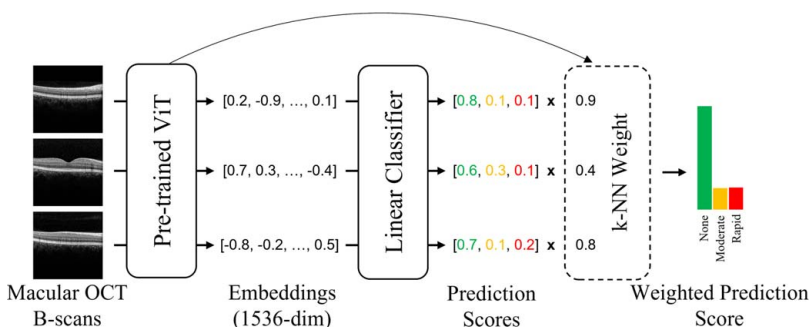


FIGURE 3. Overview of the classification pipeline. To generate a prediction for a macular OCT, the individual B-scans are each embedded using the pretrained vision transformer model. A fully connected linear classifier is trained for each prediction task (progression identification or progression prediction) and outputs prediction scores corresponding to no progression, moderate progression, and rapid progression for each B-scan. A weighted average of these prediction scores is taken using the k-nearest neighbors classifier on the glaucoma status of individual B-scans, which produces the final predictions for the macular OCT. OCT indicates optical coherence tomography.

softmax across the 3 output labels). This assigns higher weights to model predictions based on B-scans for which the pretrained ViT model was able to accurately determine glaucoma status. Intuitively, this allows the entire macular OCT study to be considered with preferential attention paid to the B-scans most relevant to glaucomatous macular changes, much as a clinician would search for abnormal patterns when examining B-scans.

Finally, these weights are used to take a weighted average of the B-scan probability scores, yielding prediction scores across the 3 output labels for the entire macular OCT study. This score was used to evaluate overall model performance and calculate area under the receiver operating characteristic curve (AUC), with 95% confidence intervals calculated by nonparametric bootstrapping.²⁰

To examine which B-scans were the most predictive of progression, B-scans for each macular OCT study were divided into quintiles from superior to inferior. For OCT studies obtained from eyes that met the criteria for rapid or moderate visual field progression, the B-scans contributing the top 20% of the progression prediction score mass were identified (separately for both before and after the k-NN reweighing), and the proportion of each quintile's B-scans thus identified was recorded. Overall differences in proportions of B-scans predictive for progression between quintiles were assessed using a χ^2 test.

RESULTS

The model pretraining process used 7,702,201 B-scan images from 151,389 macular OCT studies. The pretraining data set included a total of 1417 patients with a clinical diagnosis of POAG. These patients underwent a median of 6 HVF tests (interquartile range 2, 8) during a mean duration of HVF observation of 4.2 ± 2.2 y.

For the progression detection task, 1639 eyes met inclusion criteria, with exclusions for incisional glaucoma surgery ($n=53$), treatment with anti-VEGF agent ($n=43$), and visually significant cataract ($n=9$), resulting in 3902 macular OCT studies of 1534 eyes of 828 patients included for analysis. There were 486 (58.7%) female patients; the median follow-up was 3.4 years (IQR 2.9–4.8). Characteristics of the macular OCT studies are given in Table 1. The training validation splits contained 2478 and 620 OCT studies, respectively. The hold-out test set of 307 eyes contained 804 macular OCT studies, of which 112 and 99 were

moderately and rapidly progressing, respectively. There was no significant difference in the proportion of eyes with glaucoma in the training and validation groups. The model distinguished stable eyes from moderately or rapidly progressing eyes (Fig. 4A), achieving an AUC of 0.90 (95% CI, 0.88–0.91). At the balanced operating point, the sensitivity for detecting progression was 0.84, and the specificity was 0.82. In addition, the model detected rapid progression with an AUC of 0.92 (95% CI, 0.91–0.93) (Fig. 4B). The sensitivity for detecting rapid progression was 0.84, and the specificity was 0.87 at the balanced operating point.

For progression prediction, 1436 eyes met inclusion criteria, with exclusions for incisional glaucoma surgery ($n=48$), treatment with the anti-VEGF agent ($n=35$), and visually significant cataract ($n=7$), resulting in 1346 macular OCT imaging studies from 1205 eyes of 784 patients included for analysis. There were 469 (60.0%) female patients; the median follow-up was 3.6 years (IQR 3.0–5.1). Characteristics of the macular OCT studies are given in Table 2. The training and validation splits contained 852 and 214 OCT studies, respectively. The hold-out test set for progression prediction included 241 eyes with 280 macular OCT imaging studies, of which 39 preceded moderate and 34 preceded rapid progression. There was no significant difference in the proportion of eyes with glaucoma in the training and validation groups. The model also demonstrated a high predictive ability for forecasting future glaucoma progression (Fig. 5A), with an AUC of 0.85 (95% CI 0.83–0.87). The sensitivity was 0.82 and the specificity was 0.80 at the balanced operating point. Rapid progression was predicted with an AUC of 0.84 (95% CI 0.81–0.86), with a

TABLE 1. Patient Characteristics by Progression Status for the Detection of Concurrent Progression

	No progression	Moderate progression	Rapid progression
No. OCTs	2862	554	486
Age at baseline	67.4 ± 12.5	68.8 ± 12.1	70.0 ± 14.3
Baseline MD	-2.98 ± 3.60	-4.78 ± 4.02	-5.36 ± 3.70
MD rate of change (dB/y)	0.15 ± 0.62	-0.69 ± 0.14	-1.83 ± 0.81

IQR indicates interquartile range; MD, mean deviation; OCT, optical coherence tomography.

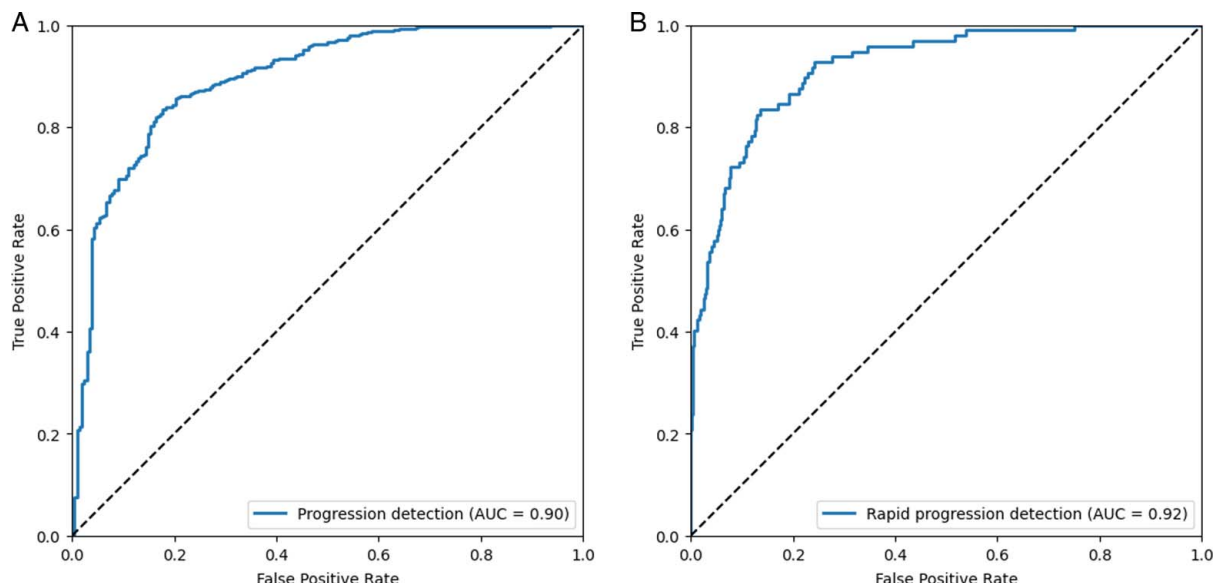


FIGURE 4. A, ROC curve for progression identification. B, ROC curve for rapid progression identification. ROC indicates receiver operating characteristic.

sensitivity of 0.75 and specificity of 0.78 at the balanced operating point (Fig. 5B).

Moreover, progression prediction was evaluated for macular OCTs obtained early (at least 6 months before future progression, $n=148$) and late (less than 6 months before future progression, $n=132$). The AUC for the early macular OCTs was 0.83 and for the late macular OCTs was 0.85.

On examination of the most relevant B-scans for progression classification, there was no significant difference found between superior-to-inferior quintiles within the macular OCT studies for progression identification or for progression prediction. This was consistent both with and without the k-NN reweighting.

To examine the impact of the k-NN weighting of the B-scan-wise linear classifier outputs, the linear classifier prediction scores were averaged without weighting. The AUC for the unweighted progression identification decreased to 0.87, and for unweighted progression prediction decreased to 0.77. The ability of the pretrained ViT embeddings to separate glaucomatous from healthy macular B-scans is illustrated using t-distributed Stochastic Neighbor Embedding (Supplementary Figure 1, Supplemental Digital Content 1, <http://links.lww.com/IJG/A869>).

DISCUSSION

The challenge of identifying glaucomatous progression remains a significant barrier to the optimal management of glaucoma. Interrogation of previously overlooked disease-

relevant structural features using deep learning has great potential to address this gap by linking structural and functional markers of progression. In addition, artificial intelligence (AI)-based tools to support clinicians in the assessment of imaging data may enhance efficiency and help compensate for variations in the levels of clinician expertise in evaluating such data. Assessment of visual function with perimetry is more time-consuming and burdensome for patients than assessment of structural measures with OCT; therefore, technological advances that allow a reduction in the reliance on and frequency of visual field testing have the potential to improve patient satisfaction. In the present study, a deep learning model used structural features of macular OCT to identify concurrent clinically significant glaucomatous visual field progression and to predict future visual field progression using only a single baseline scan.

There has been mounting evidence for the value of longitudinal macular OCT in glaucoma management. Rapid RGC complex thinning has been reported to predict central visual field loss over time,²¹ while thickness maps derived from macular OCT have been shown to distinguish glaucoma from normal with high diagnostic accuracy.^{22,23} Though most studies thus far have used macular OCT-derived parameters—namely thickness—in their analyses,²⁴ recent work has explored the use of full, unsegmented macular OCT imaging studies to detect referable glaucoma.²⁵

Increasingly, deep learning methods have enabled more sophisticated analyses supporting glaucoma management. Multiple modalities, most commonly fundus photography^{15,26}

TABLE 2. Patient Characteristics by Progression Status for the Prediction of Future Progression

	No progression	Moderate progression	Rapid progression
No. OCTs	1013	175	158
Age at baseline	66.5 ± 12.7	66.6 ± 11.5	67.7 ± 12.3
Time until first HVF (y)	0.81 ± 0.77 (IQR 0.34, 1.02)	0.60 ± 0.55 (IQR 0.18, 1.0)	0.69 ± 0.68 (IQR 0.25, 0.94)
Baseline MD	-2.52 ± 4.54	-2.64 ± 3.99	-4.06 ± 4.12

HVF indicates Humphrey Visual Field; IQR, interquartile range; MD, mean deviation; OCT, optical coherence tomography.

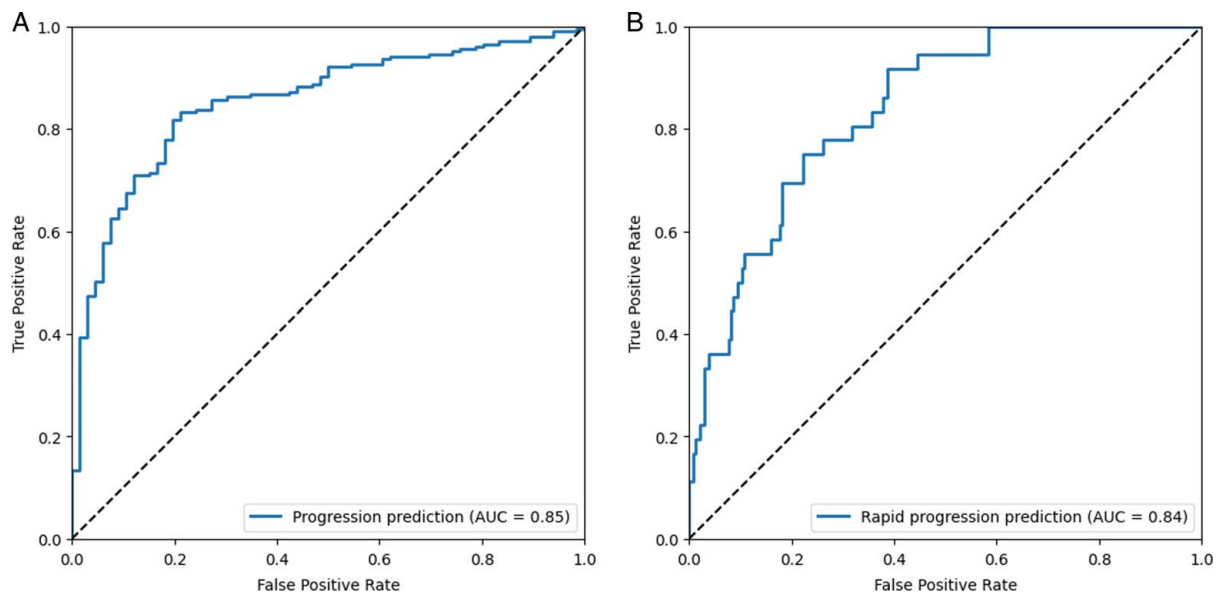


FIGURE 5. A, ROC curve for progression prediction. B, ROC curve for rapid progression prediction. ROC indicates receiver operating characteristic.

and RNFL OCT,^{27,28} have been examined to diagnose glaucoma and quantify disease severity. Deep learning is particularly well-suited to the examination of ophthalmologic imaging data, given its ability to identify patterns within imaging data that may not be immediately apparent to the human observer. More recently introduced transformer-based models have also outperformed older deep-learning methods for glaucoma classification tasks.^{24,29} Transformer models have been shown to be particularly advantageous on large-scale datasets comprising millions of images, as in the current study.³⁰ However, relatively few studies to date have used deep learning to examine the diagnostic and predictive value of macular OCT in glaucoma,^{22,23,25,31,32} and to our knowledge, this is the first to use a ViT model pretrained in a self-supervised manner such as DINO.

Detecting and predicting glaucoma progression is a more challenging problem than simply diagnosing glaucoma. The method presented in the current paper offers some key advantages to previously published approaches to OCT analysis with deep learning. First, the algorithm operates on segmentation-free data and considers all B-scans within the OCT study, providing maximal information for the model to evaluate. Moreover, the self-supervised training of the ViT model using a large quantity of macular OCT data enabled representation learning on macular OCT B-scans that generate embeddings that generalize sufficiently to downstream classification tasks. This model and strategy can also be applied to settings other than glaucoma.

The findings of this study demonstrate the feasibility of using macular OCT to detect functional glaucoma progression using structural data with reasonably high accuracy. The model identified macular OCTs obtained during periods of HVF progression of at least -0.5 dB/year, and the predictive ability further improved for detection of rapid HVF progression of at least -1 dB/year. This improvement suggests that increasing progression severity is reflected in more pronounced macular OCT changes, enabling risk stratification of patients through classification into rapidly

and moderately progressing groups. The prediction score of the model can also be varied to prioritize sensitivity or specificity, depending on the clinical needs. Moreover, the model was more predictive of future progression when given a macular OCT obtained closer in time to the progression interval. There was no significant difference in the location of B-scans most diagnostic of progression or future progression, indicating that changes throughout the macula are associated with progression.

These results build upon previous work, which has used color fundus photographs to diagnose glaucoma and predict functional progression,¹⁵ as well as another study that used circum papillary RNFL thickness measurements to detect structural progression.²⁷ While this study demonstrates promising use for macular OCT, which may be more broadly available in patients who have not yet received dedicated glaucoma evaluation, there is complementary information in fundus photography and circum papillary OCT imaging, which may yield improved insights on the disease process. As deep learning techniques continue to be developed for glaucoma applications, it is likely that methods combining information from multiple modalities, including OCT imaging data of the optic disk and circum papillary retina, will further improve the accuracy of AI models for the detection and prediction of glaucoma progression.

An important methodological aspect of this study is the use of HVF progression as a functional, rather than structural, end point. As the ultimate goal of glaucoma therapy—whether medical or surgical—is the prevention of irreversible vision loss, delivering interventions to optimize functional outcomes may result in better clinical outcomes than optimizing structural measures such as RNFL thickness, which may not directly impact patient quality of life. HVF progression, as measured by the rate of MD change, has further been validated as a strong clinically relevant end point for glaucoma progression.¹⁸ As this tool can predict progression using only 1 macular OCT in place of 5 HVF tests with an AUC of 0.849, progressing eyes can potentially

be identified earlier than would be possible using perimetry, enabling timelier intensification of therapy. Moreover, patients identified to be at high risk of future progression can be more closely monitored and potentially targeted for intensification of therapy. In this manner, the use of deep learning as a precision medicine tool has great potential to supplement clinical decision-making by providing clinicians with predictive forecasts regarding glaucoma progression and flagging patients in whom a high likelihood of concurrent visual field progression is present.

Limitations

As this was a single-center study, the generalizability of these results to other patient populations remains to be confirmed, and such studies are in the planning phase. The data set included only Spectralis OCT imaging studies; imaging from other platforms may differ systematically and require a new pretraining process. There may also be a component of selection bias in the present cohort due to the requirement of 5 HVF tests for inclusion, as patients deemed more likely to progress may have been more likely to have been under more intensive longitudinal observation and thus were more likely to have been included in this analysis. Such bias likely increased the proportion of eyes with moderate and rapid progression in both the training and testing datasets; however, we do not believe this was likely to have influenced our assessments of the diagnostic accuracy of the deep learning algorithm.

While clinically relevant, the use of HVF data as the prediction end point may not be ideal due to its high test variability. Although this limitation was mitigated by the requirement of 5 separate HVF tests with at least 6 months between tests to define progression, this strategy may also cause short, rapid periods of progression to be overlooked. For instance, a patient with rapid progression evident between the first and second HVF tests, which then stabilized between the second and fifth tests, may be categorized as being stable overall. Early pointwise HVF changes may also not be captured completely by MD changes, and other disease processes may contribute to HVF changes. More generally, further work standardizing the analysis of perimetry data to robustly quantify short-term and long-term progression or stabilization throughout the disease course will improve the ability of deep learning methods to provide clinically relevant predictions. Future efforts will be directed to explore the predictive value of macular OCT for alternative markers of glaucoma progression, such as circum-papillary RNFL thinning, using deep learning.

Finally, the explainability of the model is limited due to the multistage approach to classification. While the ability of the pretrained ViT model to cluster related images with only self-supervised training can be visualized (Supplemental Fig. 1, Supplemental Digital Content 1, <http://links.lww.com/IJG/A869>), the downstream tasks of progression detection and prediction can only be examined for relevant B-scans used in model decision-making; the relevant regions of each B-scan cannot be directly visualized. Further work that extends ViT modeling of macular OCT to a 3-dimensional framework capable of examining the entire OCT examination at once may mitigate this drawback.

CONCLUSIONS

A deep learning model detected clinically significant functional glaucoma progression using macular OCT

tomograms and was also able to predict future progression. Early identification of patients undergoing glaucoma progression or at high risk thereof may aid clinical decision-making to optimize vision preservation. Further research is needed to elucidate the structural underpinnings of glaucoma progression within the macula. Future work should be directed toward including optic disk and peripapillary OCT imaging data in deep learning models.

REFERENCES

1. Tham Y-C, Li X, Wong TY, et al. Global prevalence of glaucoma and projections of glaucoma burden through 2040: a systematic review and meta-analysis. *Ophthalmology*. 2014;121: 2081–2090.
2. Coleman AL, Miglior S. Risk factors for glaucoma onset and progression. *Survey Ophthalmol*. 2008;53(6, suppl):S3–S10.
3. Sharma P, Sample PA, Zangwill LM, et al. Diagnostic tools for glaucoma detection and management. *Survey Ophthalmol*. 2008;53(6, suppl):S17–S32.
4. Leung CK, Cheung CY, Weinreb RN, et al. Retinal nerve fiber layer imaging with spectral-domain optical coherence tomography: a variability and diagnostic performance study. *Ophthalmology*. 2009;116:1257–1263.e1252.
5. Medeiros FA, Zangwill LM, Bowd C, et al. The structure and function relationship in glaucoma: Implications for detection of progression and measurement of rates of change. *Invest Ophthalmol Visual Sci*. 2012;53:6939–6946.
6. Mwanza J-C, Kim HY, Budenz DL, et al. Residual and dynamic range of retinal nerve fiber layer thickness in glaucoma: Comparison of three OCT platforms. *Invest Ophthalmol Visual Sci*. 2015;56:6344–6351.
7. Saunders LJ, Medeiros FA, Weinreb RN, et al. What rates of glaucoma progression are clinically significant? *Expert Rev Ophthalmol*. 2016;11:227–234.
8. Spry PGD, Johnson CA, McKendrick AM, et al. Variability components of standard automated perimetry and frequency-doubling technology perimetry. *Invest Ophthalmol Visual Sci*. 2001;42:1404–1410.
9. Gardiner SK, Mansberger SL, Fortune B. Time lag between functional change and loss of retinal nerve fiber layer in glaucoma. *Invest Ophthalmol Visual Sci*. 2020;61:5–5.
10. Kim JH, Rabiolo A, Morales E, et al. Risk factors for fast visual field progression in glaucoma. *Am J Ophthalmol*. 2019; 207:268–278.
11. Sung KR, Wollstein G, Kim NR, et al. Macular assessment using optical coherence tomography for glaucoma diagnosis. *Br J Ophthalmol*. 2012;96:1452.
12. Grewal DS, Tanna AP. Diagnosis of glaucoma and detection of glaucoma progression using spectral domain optical coherence tomography. *Curr Opinion Ophthalmol*. 2013;24:150–161.
13. Mohammadzadeh V, Fatehi N, Yarmohammadi A, et al. Macular imaging with optical coherence tomography in glaucoma. *Survey Ophthalmol*. 2020;65:597–638.
14. Sung KR, Sun JH, Na JH, et al. Progression detection capability of macular thickness in advanced glaucomatous eyes. *Ophthalmology*. 2012;119:308–313.
15. Li F, Su Y, Lin F, et al. A deep-learning system predicts glaucoma incidence and progression using retinal photographs. *J Clin Invest*. 2022;132.
16. Caron M, Touvron H, Misra I, et al. Emerging Properties in Self-Supervised Vision Transformers. 2021.
17. Huang S-C, Pareek A, Jensen M, et al. Self-supervised learning for medical image classification: a systematic review and implementation guidelines. *npj Digital Medicine*. 2023;6:74.
18. Medeiros FA, Jammal AA. Validation of rates of mean deviation change as clinically relevant end points for glaucoma progression. *Ophthalmology*. 2023;130:469–477.
19. Raschka S. Model evaluation, model selection, and algorithm selection in machine learning. *CoRR*. 2018;abs/1811:12808.

20. Chihara LM, Hesterberg TC. *Mathematical statistics with resampling and R*. John Wiley & Sons; 2022.
21. Mahmoudinezhad G, Moghimi S, Nishida T, et al. Association between rate of ganglion cell complex thinning and rate of central visual field loss. *JAMA Ophthalmol*. 2023;141:33–39.
22. Asaoka R, Murata H, Hirasawa K, et al. Using deep learning and transfer learning to accurately diagnose early-onset glaucoma from macular optical coherence tomography images. *Am J Ophthalmol*. 2019;198:136–145.
23. An G, Omodaka K, Hashimoto K, et al. Glaucoma diagnosis with machine learning based on optical coherence tomography and color fundus images. *J Healthcare Engin*. 2019;2019:4061313.
24. Thompson AC, Falconi A, Sappington RM. Deep learning and optical coherence tomography in glaucoma: Bridging the diagnostic gap on structural imaging. *Front Ophthalmol*. 2022; 2:937205.
25. Russakoff DB, Mannil SS, Oakley JD, et al. A 3D deep learning system for detecting referable glaucoma using full OCT macular cube scans. *Transl Vision Sci Technol*. 2020;9: 12–12.
26. Phene S, Dunn RC, Hammel N, et al. Deep learning and glaucoma specialists: The relative importance of optic disc features to predict glaucoma referral in fundus photographs. *Ophthalmology*. 2019;126:1627–1639.
27. Mariottini EB, Datta S, Shigematsu LS, et al. Deep learning–assisted detection of glaucoma progression in spectral-domain OCT. *Ophthalmol Glaucoma*. 2023;6:228–238.
28. Hemelings R, Elen B, Barbosa-Breda J, et al. Pointwise visual field estimation from optical coherence tomography in glaucoma using deep learning. *Translational Vision Science & Technology*. 2022;11:22–22.
29. Fan R, Alipour K, Bowd C, et al. Detecting glaucoma from fundus photographs using deep learning without convolutions: Transformer for improved generalization. *Ophthalmol Science*. 2023;3:100233.
30. Dosovitskiy A, Beyer L, Kolesnikov A, et al. An Image is Worth 16x16 Words: Transformers for Image Recognition at Scale. 2021.
31. Lee J, Kim YK, Park KH, et al. Diagnosing glaucoma with spectral-domain optical coherence tomography using deep learning classifier. *J Glaucoma*. 2020;29:287–294.
32. Kim KE, Kim JM, Song JE, et al. Development and validation of a deep learning system for diagnosing glaucoma using optical coherence tomography. *J Clin Med*. 2020;9:2167.